

All-optical dynamic correction of distorted communication signals using a photorefractive polymeric hologram

Guoqiang Li,^{a)} Muhsin Eralp, Jayan Thomas, Savaş Tay, Axel Schülzgen, Robert A. Norwood, and N. Peyghambarian

Optical Sciences Center, University of Arizona, Tucson, Arizona 85721

(Received 21 October 2004; accepted 1 March 2005; published online 11 April 2005)

All-optical real-time dynamic correction of wave front aberrations for image transmission is demonstrated using a photorefractive polymeric hologram. The material shows video rate response time with a low power laser. High-fidelity, high-contrast images can be reconstructed when the oil-filled phase plate generating atmospheric-like wave front aberrations is moved at 0.3 mm/s. The architecture based on four-wave mixing has potential application in free-space optical communication, remote sensing, and dynamic tracking. The system offers a cost-effective alternative to closed-loop adaptive optics systems. © 2005 American Institute of Physics. [DOI: 10.1063/1.1898432]

Laser communication systems are attractive since they possess higher information bandwidth and security than radio-frequency systems. However, atmospheric turbulence perturbs phase and cause intensity scintillation on the detectors. The scintillation reduces the information capacity and increases the bit error rate. Adaptive optics technology can dynamically correct the spatial aberrations in the transmitted beam and significantly improve the performance.¹ A typical adaptive optics system² includes a wave front sensor for measurement of the aberrations, an actuator for wave front correction, and associated control electronics. Implementation of such a system is expensive and complex. Considerable research efforts have been devoted to real-time, low-cost adaptive optical systems. A simplified system that combines the actuator and the blind optimization algorithm has been proposed.³ The other approach uses nonlinear optical effects such as phase conjugation and multiple wave mixing.^{4–13} Photorefractive (PR) dynamic holographic techniques are of interest for laser communication since fast, low-cost, and all-optical compensation of wave front distortion can be achieved without expensive actuators, intensive computation, and complex subsystems. PR materials consist of mainly two classes: inorganic crystals and organic polymers. Phase conjugation in various PR crystals has been investigated intensively.^{4–9} However, most of the crystals are sensitive only in the visible region and are difficult to grow and polish. In contrast, PR polymers have advantages such as low cost, ease of fabrication tunability, and flexibility of synthesis. They have demonstrated response times in the millisecond range,¹⁴ near 100% diffraction efficiency,¹⁵ high coupling gain coefficients,¹⁶ near-infrared sensitivity^{17,18} and are an increasingly viable alternative to PR crystal.¹⁹ In this letter, we present high-quality dynamic correction of atmospheric-like wave front distortions using a PR polymer composite.

Various optical systems using PR holograms for real-time wave front compensation can be designed for communication links, depending on the target application. Here, we use a typical system that employs a modulated phase conjugate mirror as a remote sensor for free-space

communication.²⁰ As shown in Fig. 1(a), consider two communication stations with the objective being to communicate from station 2 to station 1. Station 1 has a light source and a receiver, whereas station 2 has a modulator and a phase conjugate mirror. The communication link can be completed in the following steps: station 1 sends a laser beacon beam to the vicinity of station 2; when receiving the light from station 1, station 2 encodes the signal to be communicated onto the modulator; the encoded beam is redirected to station 1 using phase conjugation and detected by the receiver. Although the turbulent atmosphere adds distortion to the beam, station 1 can always receive the correct signal from station 2. In addition, because of the real-time characteristic of the dynamic phase conjugate mirror, even if both stations are mobile, the communication link can still be maintained. In order to demonstrate dynamic distortion correction for this link, a system shown in Fig. 1(b) has been designed and implemented as a preliminary proof-of-principle experiment. Experiments have been done at 633 nm and extension to near IR is straightforward using PR polymers operating near 1 μm and 1.55 μm .^{17,18} As shown in Fig. 1(b), the beam

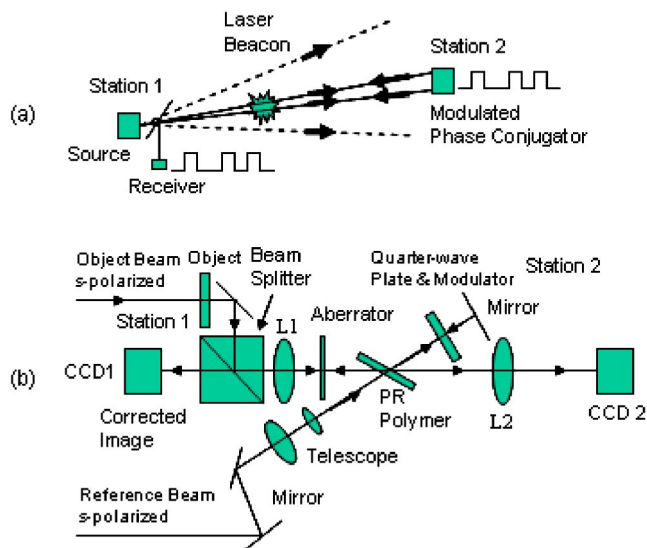


FIG. 1. (Color online) (a) Free-space remote communication link. (b) Schematic diagram of the experiment setup.

^{a)}Electronic mail: gli@optics.arizona.edu

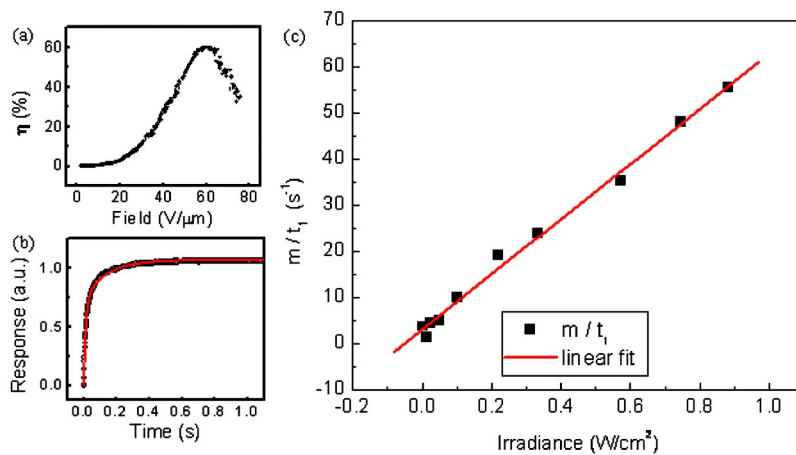


FIG. 2. (Color online) Optical property of the PR material. (a) Field dependent steady-state diffraction efficiency. (b) An example of the transient response of the diffracted signal. (c) Sensitivity of the material quantified as the intensity dependence of the speed m/t_1 (filled squares). Solid line is a linear fit.

from a He–Ne laser is vertically (s) polarized, spatially filtered, and collimated. The collimated beams are split into two arms, the object arm and the reference arm. The reference beam is directed to the PR polymer film using a reducing telescope. In the object arm, a Fourier transform lens is introduced and the PR polymer film is placed in the focal plane of the lens. The spatial spectrum of the object beam is overlapped with the reference beam in the PR polymer and a volume hologram is recorded when an appropriate voltage is applied to the PR polymer. An aberrator is placed between the lens and the PR polymer to intentionally distort the beam. In order to obtain the maximum diffraction efficiency, the PR polymer film is aligned in a tilted structure and a p -polarized beam is used to read the hologram. The angle between the two writing beams is 22° and the normal to the sample and the bisector of the two writing beams form an angle of 55° . A quarter wave plate is utilized to convert the s -polarized beam to a p -polarized beam when the beam double passes it. The reading beam is counterpropagating to the reference beam, generating a phase conjugate object beam. When the phase-conjugate object beam passes through the aberrator again, a corrected image is obtained at station 1.

A PR polymer composite PATPD:DBDC:ECZ:C₆₀ (49.5:30:20:0.5 wt %) was used, containing the charge transport polymer PATPD with polyacrylate backbone and the well-known hole-transporting tetraphenyldiaminobiphenyl-type (TPD) pendant group attached through an alkoxy linker, the nonlinear optical chromophore 3-(N,N-di-n-butylaniline-4-yl)-1-dicyanomethylidene-2-cyclohexene (DBDC), the plasticizer 9-ethylcarbazole (ECZ), and the sensitizer C₆₀. The device was fabricated by melting the material in between two indium tin oxide-coated glass with 105 μm spacers. Samples prepared in this fashion have not undergone degradation in optical quality or material properties because of crystallization even after 18 months at room temperature from the time of assembly. The glass-transition temperature T_g of the material was 43 $^\circ\text{C}$. The ability of the chromophores to reorient under the influence of an electric field at room temperature was confirmed using transient ellipsometry experiments.

For dynamic aberration correction, two of the most important performance parameters of the holographic material are response time and diffraction efficiency. Figure 2 shows the properties of the composite PATPD:DBDC:ECZ:C₆₀ measured with a four-wave mixing experiment. The field-dependent steady-state diffraction efficiency is shown in Fig. 2(a). The two s -polarized writing beams have equal fluences

of 0.55 W/cm 2 . The material showed a fast response time less than 20 ms and an external diffraction efficiency (the ratio of the diffracted signal energy to the incident beam energy) higher than 60%. The overmodulation diffraction efficiency occurred at about 60 V/ μm and, hence, in the following experiments the external field was fixed to this value. For a low T_g PR material, the refractive index modulation has two contributions. One is the Pockels electro-optic effect, the other is the spatially modulated birefringence due to the periodic poling of the nonlinear optical chromophore with the total poling field being the superposition of the internal space-charge field and the external field. The inverse of the fast response time (t_1^{-1}) of the material reflects the buildup speed of the internal space-charge field, which consists of charge generation, transportation, and trapping. Charge generation and transport are quantified in photoconductivity σ_{ph} , which is defined as

$$\sigma_{\text{ph}} = ne\mu = \frac{\phi\alpha I\tau}{h\nu} e\mu, \quad (1)$$

where n is the density of charge carriers, e is the elementary charge, μ is the mobility, ϕ is the charge generation quantum efficiency, α is the absorption coefficient, I is the intensity of the incident beam, τ is the time constant for transport, h is Planck's constant, and ν is the frequency of the light. The speed of space-charge field formation is therefore dependent on the optical intensity. The intensity dependence of the speed reflects the sensitivity of the material and can be characterized by a series of transient measurements at different intensity values. Figure 2(b) is an example of the transient response, where the total intensity of the writing beams is about 0.86 W/cm 2 . In each case, the response time constants t_1 (fast response time) and t_2 (slow response time), and the fitting parameter m are obtained by fitting the transient response of the grating to the sum of two exponentials.¹⁶ The speed of the material is measured in terms of m/t_1 . The intensity dependent speed of the material is depicted in Fig. 2(c). It is seen that the speed is almost linear in the incident intensity as predicted by Eq. (1). Video-rate response time can be obtained when the intensity is above 0.5 W/cm 2 .

The performance of our system was first verified without aberrators. The reconstructed image [taken with a charge coupled device (CCD) camera CCD1] has contrast as high as that of the transmitted image (taken with a CCD2). In order to demonstrate the capability of our system to perform high-quality correction of large aberrations, we inserted a glass

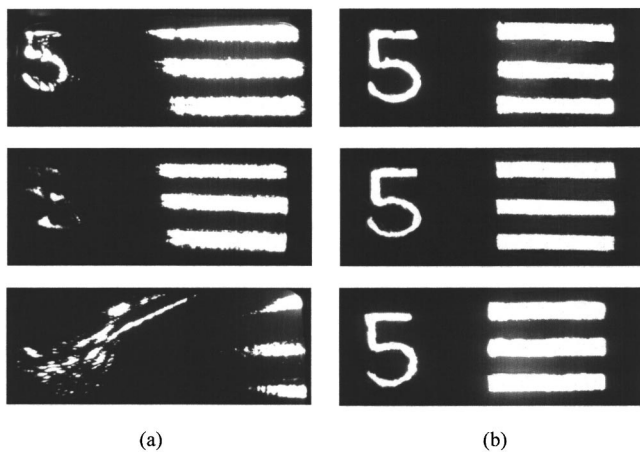


FIG. 3. (Color online) Correction of severely distorted images. (a) Distorted images. (b) Corrected images.

Petri dish (which causes large phase distortions) behind the Fourier transform lens and compare the distorted image in the transmission path and the restored image with different phase distortions. In Fig. 3, three examples are illustrated. The left column shows the distorted images and the right column shows the corresponding corrected images. The phase distortion is varied by letting the object beam transmit through different positions of the deformed glass. From top to the bottom, the transmitted images are distorted to an increasing extent. The image at the bottom left is severely distorted and the number “5” cannot be recognized at all. It is clearly seen that in all cases the phase distortion is compensated successfully and the restored images have as high a contrast as the images when no aberrator is present. We have also performed a high-quality image correction experiment using an oil-filled phase plate²¹ which generates atmospheric-like wave front aberrations. The aberrations produced by this phase plate are smaller than those of the Petri dish, but they have a higher spatial frequency reflecting the correct statistics of atmospheric turbulence. In order to demonstrate dynamic correction of the phase distortion, a stepper motor is used to move the aberrator continuously in the direction perpendicular to the signal beam propagation. We have successfully performed the experiments and videos of dynamically corrected images were obtained. Using the oil-filled phase plate, videos were taken when the aberrator was moved at 0.3 mm/s. On the other hand, when the object is moved at the same speed, the corrected images can also be dynamically refreshed without distortions.

In summary, we have demonstrated a low-cost, high-performance holographic wave front aberration correction system using a PR polymer composite. Dynamic correction of significantly distorted images can be achieved. Using the oil-filled phase plate as the aberrator, which produces atmospheric-like wave front aberrations, high quality images can be reconstructed even when the phase plate is moved at

0.3 mm/s. The technique has potential applications in remote sensing, and dynamic tracking. By using phase conjugate modulation of the reading beam, it can also be used for the correction of aberrations encountered in free-space digital optical communication. Future work will extend the working wavelength of the system to near-infrared region.

The authors would like to acknowledge support from the Air Force Office of Scientific Research under Contract No. FA9550-04-1-0096, and the State of Arizona TRIF Photonics program. The authors thank Dr. Michael Lloyd-Hart of the Department of Astronomy at the University of Arizona for providing the oil-filled phase plate, and also thank Mr. Canek Fuentes-Hernandez and Dr. Raymond Kostuk for discussions.

¹B. M. Levine, E. A. Martinsen, A. Wirth, A. Jankevics, M. Toledo-Quinones, F. Landers, and T. L. Bruno, *Appl. Opt.* **37**, 4553 (1998).

²R. K. Tyson and D. E. Canning, *Appl. Opt.* **42**, 4239 (2003).

³T. Weyrauch, M. A. Vorontsov, J. W. Gowens, and T. G. Bifano, *Proc. SPIE* **4489**, 177 (2002); M. L. Plett, P. R. Barbier, and D. W. Rush, *Appl. Opt.* **40**, 327 (2001).

⁴*Landmark Papers on Photorefractive Nonlinear Optics*, edited by P. Yeh and C. Gu (World Scientific, NJ, 1995).

⁵*Photorefractive Optics: Materials, Properties, and Applications*, edited by F. T. S. Yu and S. Yin (Academic, San Diego, 2000).

⁶*Holographic Data Storage*, edited by H. Coufal, D. Psaltis, and G. Sincerbox (Springer, New York, 2000).

⁷A. E. Chiou and P. Yeh, *Opt. Lett.* **11**, 461 (1986).

⁸I. Semenova, S. Dimakov, and G. Dreiden, *Proc. SPIE* **4416**, 162 (2001).

⁹M. P. Bogdanov, S. A. Dimakov, A. V. Gorlanov, V. M. Jrtuganov, S. I. Klimentev, K. G. Lazunin, I. B. Orlova, A. M. Scott, V. E. Sherstobitov, N. A. Svetsitskaya, and D. I. Zhuk, *Proc. SPIE* **3263**, 2 (1998).

¹⁰E. N. Leith and J. Upatnieks, *J. Opt. Soc. Am.* **56**, 523 (1966); H. Kogelnik and K. S. Pennington, *ibid.* **58**, 273 (1968); A. Yariv, *Appl. Phys. Lett.* **28**, 88 (1976).

¹¹N. Kukhtarev, B. S. Chen, H. J. Caulfield, and P. Venkateswaru, *Proc. SPIE* **2003**, 56 (1993); S. Weiss, M. Segev, S. Sternklar, and B. Fischer, *Appl. Opt.* **27**, 3422 (1988); S. H. Chakmakjian, M. T. Gruneisen, K. Koch, M. A. Kramer, and V. Esch, *ibid.* **34**, 1076 (1995).

¹²A. N. Simonov, A. V. Larichev, V. P. Shibaev, and A. I. Stakhanov, *Opt. Commun.* **197**, 175 (2001); W.-J. Joo, N.-J. Kim, H. Chun, I. K. Moon, and N. Kim, *Polymer* **42**, 9863 (2001).

¹³J. G. Winiazar and F. Ghebremichael, *Appl. Opt.* **43**, 3166 (2004); J. G. Winiazar, F. Ghebremichael, J. Thomas, G. Meredith, and N. Peyghambarian, *Opt. Express* **12**, 2517 (2004).

¹⁴J. A. Herlocker, K. B. Ferrio, E. Hendrickx, B. D. Guenther, S. Mery, B. Kippelen, and N. Peyghambarian, *Appl. Phys. Lett.* **74**, 2253 (1999).

¹⁵K. Meerholz, B. L. Volodin, Sandalphon, B. Kippelen, and N. Peyghambarian, *Nature (London)* **371**, 497 (1994).

¹⁶D. Wright, U. Gubler, Y. Roh, W. E. Moerner, M. He, and R. J. Twieg, *Appl. Phys. Lett.* **79**, 4274 (1999).

¹⁷M. Eralp, J. Thomas, S. Tay, G. Li, G. Meredith, A. Schülzgen, N. Peyghambarian, and S. R. Marder, *Appl. Phys. Lett.* **85**, 1095 (2004).

¹⁸S. Tay, J. Thomas, M. Eralp, G. Li, B. Kippelen, S. R. Marder, G. Meredith, A. Schülzgen, and N. Peyghambarian, *Appl. Phys. Lett.* **85**, 4561 (2004).

¹⁹B. L. Volodin, B. Kippelen, K. Meerholz, B. Javidi, and N. Peyghambarian, *Nature (London)* **383**, 58 (1996).

²⁰G. J. Gaeta and D. M. Pepper, *Opt. Lett.* **16**, 802 (1991).

²¹T. A. Rhoadarmer and J. R. P. Angel, *Appl. Opt.* **40**, 2946 (2001).